Integrated optical distributed feedback laser with Ti:Fe:Er:LiNbO 3 waveguide

B. K. Das, R. Ricken, and W. Sohler

Citation: Applied Physics Letters **82**, 1515 (2003); doi: 10.1063/1.1559443
View online: http://dx.doi.org/10.1063/1.1559443
View Table of Contents: http://scitation.aip.org/content/aip/journal/apl/82/10?ver=pdfcov
Published by the AIP Publishing

Integrated optical distributed feedback laser with Ti:Fe:Er:$LiNbO_3$ waveguide

B. K. Das,[a] R. Ricken, and W. Sohler
Department of Applied Physics, University of Paderborn, Warburger Strasse 100 D-33098, Paderborn, Germany

(Received 9 October 2002; accepted 8 January 2003)

A distributed feedback (DFB) laser in $LiNbO_3$ is demonstrated using a Ti:Fe:Er:$LiNbO_3$ waveguide with a holographically written photorefractive grating. The DFB laser was combined with a waveguide amplifier on the same substrate. Up to 1.12 mW of output power at $\lambda = 1531.35$ nm was emitted by the laser/amplifier combination at a pump power level of 240 mW ($\lambda_P = 1480$ nm). The emission spectrum consists of the two lowest-order DFB modes of about 3.9 GHz frequency spacing. Whereas the measured threshold gain of ~ 3.3 dB/cm approximately agreed with the modeling results, the observed mode spacing was clearly smaller than calculated. © *2003 American Institute of Physics.* [DOI: 10.1063/1.1559443]

Recently, distributed Bragg reflector (DBR) lasers were developed in $LiNbO_3$ with a Ti-indiffused waveguide. Their cavity consists of a thermally fixed, photorefractive Bragg grating in a Fe-doped section near one end face, an Er-doped amplifier section in the middle, and a broadband dielectric mirror deposited on the other end face.[1] Single-frequency DBR-laser emission was also demonstrated in Ti:Er:$LiNbO_3$, with a cavity comprised of two fixed photorefractive gratings fabricated in Fe-doped regions on both sides of the Er-doped gain section.[2] The spectral linewidth of such DBR lasers can be as low as 10 kHz.[3] Therefore, these lasers are attractive for wavelength division multiplex systems and for interferometric instrumentation.

However, up to now there has been no report in the literature on a distributed feedback (DFB) laser in $LiNbO_3$, although it might be even more attractive than a DBR structure due to its shorter length and therefore better integrability. The development of a DFB laser requires low loss waveguides, high optical gain, and strong optical feedback in the grating structure. By using Ti-indiffused waveguides in a laser-active, Er-diffusion doped $LiNbO_3$ substrate, co-doped with Fe to enable the fabrication of a photorefractive grating, it was possible to meet these requirements and to develop an integrated optical DFB laser in $LiNbO_3$ (see Fig. 1). Its fabrication and properties are reported in this letter together with a theoretical analysis.

The laser was fabricated in the surface of a 50-mm-long, 12-mm-wide, and 1-mm-thick, optical grade X-cut $LiNbO_3$ crystal with the optical (z)-axis aligned parallel to the direction of the optical waveguide. The fabrication essentially consists of a sequence of three diffusion steps for erbium, iron, and titanium before the photorefractive grating is defined. As the diffusivity of erbium is the lowest of all these dopants, it was indiffused first to get a laser-active surface layer. A 19-nm-thick erbium layer was vacuum-deposited on the whole surface of the sample and then indiffused at 1130 °C for 120 h. This results in a Gaussian concentration profile with a calculated diffusion depth of 4.4 μm and a surface concentration of 1.8×10^{20} cm^{-3}. Subsequently, to create photorefractive centers, a 32-nm-thick, vacuum-deposited Fe layer of 20-mm width was indiffused at 1060 °C during 72 h on the right side of the sample (see Fig. 1). In this way, a very deep concentration profile is obtained with a nearly constant Fe concentration of 6.0×10^{19} cm^{-3} in the Er-doped layer.

Finally, a 7-μm-wide and 103-nm-thick, photolithographically defined Ti-stripe parallel to the z-axis was indiffused at 1060 °C for 7.5 h to form the optical channel (single-mode in the range $1470\ \text{nm} < \lambda < 1580$ nm). The polarization independent mode-size ($1/e$) and the scattering losses of a reference waveguide without Er doping on the same sample were measured to be $\sim 7.0\times4.5\ \mu m^2$ and ~ 0.15 dB/cm, respectively, at a 1550-nm wavelength.

The sample was then annealed at 500 °C for 6 h in a reducing wet atmosphere to enhance the Fe^{2+}/Fe^{3+} ratio (>0.1) and the proton concentration in the surface layer of the Fe-doped section. This helps to fabricate an efficient photorefractive grating in a short time (see next section). Afterwards, both polished end faces were antireflection-coated for $\lambda \sim 1550$ nm.

From DFB-laser modeling, we learned that both the optical gain and the feedback in the amplifying grating structure should be as high as possible to get an acceptable laser threshold. We therefore decided to write the DFB grating in the Fe-doped section for a Bragg wavelength of 1531 nm, where the optical gain in the Er-doped waveguide can even

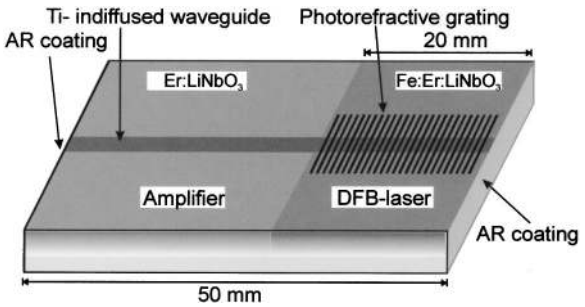

FIG. 1. Schematic structure of the Ti:Fe:Er:$LiNbO_3$ DFB laser with integrated Er-doped amplifier. AR: antireflection.

[a]Electronic mail: b.das@physik.uni-paderborn.de

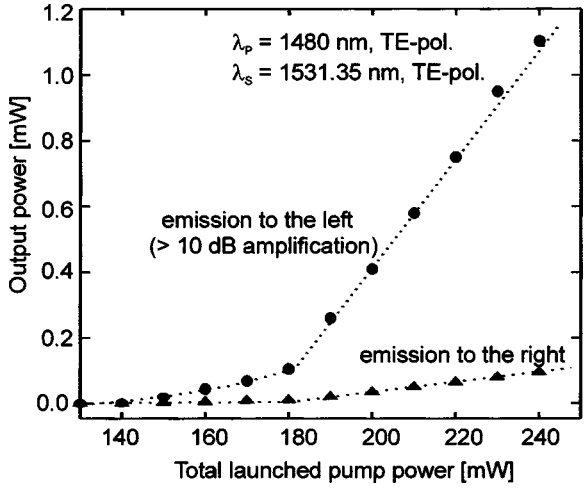

FIG. 2. Laser output power emitted to the right (without additional amplification) and to the left (after passing the waveguide amplifier) versus total launched pump power.

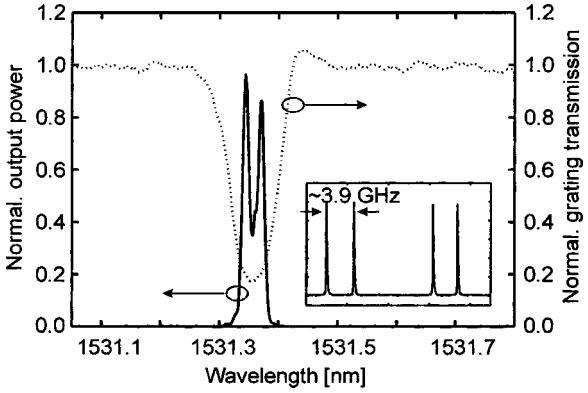

FIG. 3. Laser emission spectrum measured with an optical spectrum analyzer of 10-pm resolution, together with the normalized grating transmission (dotted line). Inset: High-resolution emission spectrum measured with a scanning Fabry–Perot resonator of 15-GHz free spectral range.-

exceed 3 dB/cm sufficient pump power provided. This requires a grating periodicity of ~345 nm. In a holographic setup (described in more detail in Ref. 2), the grating was written using an argon-ion laser ($\lambda = 488$ nm, $P = 1$ W). After an exposure time of only 2 min, the grating peak reflectivity exceeded 90%; the linewidth of the spectral grating response measured in transmission was ~85 pm (~10.9 GHz) (see dotted line in Fig. 3). Such an index grating generated by the light-induced periodic space-charge field via the electro-optic effect is volatile; it decays with time after switching off the holographic illumination. Therefore, fixed gratings were also developed in a Ti:Fe:Er:$LiNbO_3$ surface. They were fabricated at elevated temperatures ($T \sim 180\,^{\circ}$C) to get a higher proton mobility, leading to an ionic compensation of the original light-induced space-charge distribution.[4] After cooling to room temperature, they were uniformly illuminated by argon laser light ($\lambda = 488$ nm, $I = 250$ mW/cm^2) or by an array of blue light emitting diodes to develop the fixed ionic grating. This induces a phase-shifted replica of the index grating generated by the original periodic space-charge distribution.[4] However, as a reflectivity >80% was necessary to achieve lasing, fixed (ionic) photorefractive gratings could not yet be used; their maximum reflectivity was lower than 80%.

The pump light ($\lambda_P = 1480$ nm, TE polarization) of two laser diodes was coupled from the right- and left-hand sides into the waveguide structure during holographic exposure for grating definition. Fiberoptic wavelength multiplexers allowed extracting the laser emission, which sets in at a launched pump power level of about 175 mW. The maximum of the output power emitted to the right was ~95 μW at about 240 mW total launched pump power. At the same pump power level, 1.12 mW was emitted to the left, thanks to the optical gain of more than 10 dB in the ~32-mm-long, Er-doped waveguide amplifier on the left of the DFB structure. Fig. 2 gives the power characteristics of the laser.

The emission wavelength of the laser was ~1531.35 nm, clearly determined by the grating characteristics. The two distinguished DFB modes in the emission spectrum could already be resolved with an optical spectrum analyzer of 10-pm resolution; their wavelength separation is ~29 pm (3.7 GHz). The emission spectrum is shown in Fig. 3, together with the grating response. It is evident that the two emission lines arise symmetrically on both sides of the peak reflectivity. The separation of the two emission frequencies was even better resolved with a scanning Fabry–Perot spectrum analyzer; a figure of ~3.9 GHz was measured. Besides emission of both DFB modes in TE polarization, emission in TM polarization was sometimes observed as well. The cause of the polarization flipping is not yet understood. However, stabilization of one of both states of polarization would be easy by intracavity integration of a (low extinction) polarizer.

Coupled mode analysis allowed us to investigate theoretically the threshold gain of the laser and the frequency spacing of the DFB modes. The reflectivity R of an amplifying integrated optical DFB structure of length L and uniform coupling coefficient κ due to the periodic refractive index perturbation can be written as a function of the optical gain g of the medium and the frequency ν:[5]

$$R(g,\nu) = \left| \frac{i\kappa \sinh(\gamma\ L)}{i\gamma \cosh(\gamma\ L) - [\delta + i(g-\alpha)]\sinh(\gamma\ L)} \right|^2, \tag{1}$$

with $\gamma = \sqrt{\kappa^2 + [(g-\alpha) - i\delta]^2}$, $\delta = [2\pi n_{\mathrm{eff}}(\nu - \nu_B)]/c$; n_{eff} and α are the effective refractive index and loss coefficient of the Ti:Fe:Er:$LiNbO_3$ single-mode waveguide, respectively, and ν_B is the Bragg frequency of the photorefractive grating; c is the vacuum velocity of light. It is evident from Eq. (1) that the laser threshold corresponds to the singularities of its right-hand side leading to the condition

$$i\gamma \cosh(\gamma\ L) - [\delta + i(g-\alpha)]\sinh(\gamma\ L) = 0. \tag{2}$$

The values of κ, n_{eff}, ν_B, etc., were evaluated from the measured grating response, allowing us to plot contours of constant reflectivity R in the plane of $\{g, \nu - \nu_B\}$ (see Fig. 4). Three pairs of singularities are observed close to the Bragg frequency. The threshold gain for the simultaneous oscillation of the two lowest-order DFB modes is about 4 dB/cm, slightly higher than observed experimentally. This can be understood by the influence of amplified spontaneous emission in the integrated amplifier section emitted into the DFB

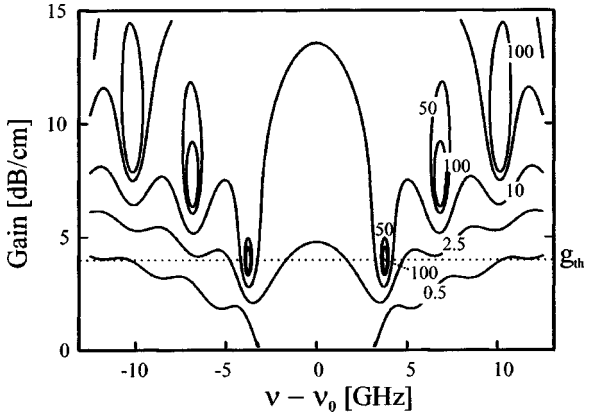

FIG. 4. Contours of constant reflectivity of the amplifying grating in the plane of optical gain g and frequency spacing from the Bragg frequency $\{\nu-\nu_B\}$, obtained by coupled mode theory. g_{th} is the threshold gain for the lowest-order DFB modes.

structure.[6] The theoretical mode frequency spacing is about 6.4 GHz, which is essentially larger than the experimental result of 3.9 GHz.

In summary, an integrated optical DFB laser in $LiNbO_3$ was demonstrated with a photorefractive grating in a Ti:Fe:Er:$LiNbO_3$ waveguide. It is combined with a waveguide amplifier on the same substrate. The laser emission spectrum at 1531.35 nm consists of the two specific DFB modes of narrow linewidth and ~3.9-GHz separation.

It should also be possible to develop fixed photorefractive gratings of stronger feedback (higher reflectivity) in the Er-doped section to obtain stable laser operation without permanent holographic illumination. Moreover, even single-frequency emission can be achieved by introducing a $\pi/2$ phase shift in the middle of the DFB grating, or by using a coupled-cavity design of DFB and DBR lasers, which also lowers the threshold pump power considerably. The second approach has recently been demonstrated experimentally.[7]

This work has been supported by the Deutsche Forschungsgemeinschaft as one project of the research group "Integrated Optics in Lithium Niobate: New Devices, Circuits and Applications."

[1] C. Becker, A. Greiner, T. Oesselke, A. Pape, W. Sohler, and H. Suche, Opt. Lett. **23**, 1194 (1998).
[2] B. K. Das, H. Suche, and W. Sohler, Appl. Phys. B: Lasers Opt. **73**, 439 (2001).
[3] I. Baumann, S. Bosso, R. Brinkmann, R. Corsini, M. Dinand, A. Greiner, K. Schäfer, J. Söchtig, W. Sohler, H. Suche, and R. Wessel, IEEE J. Sel. Top. Quantum Electron. **2**, 355 (1996).
[4] K. Buse, S. Breer, K. Peithmann, S. Kapphan, M. Gao, and E. Krätzig, Phys. Rev. B **56**, 1225 (1997).
[5] A. Yariv, *Quantum Electronics* (Wiley, New York, 1988), Chap. 22.
[6] S. Wang, R. F. Cordero, and C. Tseng, J. Appl. Phys. **45**, 3975 (1974).
[7] B. K. Das, R. Ricken, V. Quiring, H. Suche, and W. Sohler, *Proc. European Conference on Optical Communication 2002*, Copenhagen, Denmark, (2002), Vol. 4, Paper 11.2.2.